Electronic structure of $Yb_{2.75}C_{60}$

Hongnian Li, Shaolong He, Hanjie Zhang, Bin Lu, Shining Bao, Haiyang Li, Pimo He, and Yabo Xu
Department of Physics, Zhejiang University, Hangzhou 310027, People's Republic of China

Tianliang Hao
The Central Laboratory, Zhejiang University, Hangzhou 310027, People's Republic of China
(Received 11 March 2003; revised manuscript received 25 August 2003; published 28 October 2003)

Ultraviolet photoemission spectra of $Yb_{2.75}C_{60}$ thin films are measured. The valence band is a wide hump centered at ~0.8 eV below the Fermi level. The result also indicates the semiconducting property of $Yb_{2.75}C_{60}$ since no Fermi edge is observed. The hybridization between 6*s* states of Yb and the lowest-unoccupied-molecular-orbital (LUMO) band of C_{60} is non-negligible although it should not be considered to be strong. More than 14% of Yb 6*s* electrons are estimated to be distributed in the covalent bonds between Yb and C_{60}. The spectra for submonolayer C_{60} on Yb film reveal that Yb 6*s* electrons can easily transfer to C_{60} and such demonstrate that the bonding in $Yb_{2.75}C_{60}$ is mainly ionic. The LUMO+1 orbital of the submonolayer C_{60} is partially occupied, which is different from the case in $Yb_{2.75}C_{60}$. There is no evidence of trivalent Yb in the spectra.

DOI: 10.1103/PhysRevB.68.165417 PACS number(s): 71.20.Tx, 73.20.At, 73.61.Wp

I. INTRODUCTION

The electronic structure of the rare-earth-doped fulleride, $Yb_{2.75}C_{60}$, deserves close attention due to the nonintegral stoichiometry, which was not observed in the alkali-metal-doped and alkaline-earth-metal-doped fullerides. More importantly, knowledge of the electronic states near Fermi level is the foundation of understanding physical properties (including the possible superconductivity[1,2] at ~6 K) of $Yb_{2.75}C_{60}$. The photoemission spectroscopic (PES) technique is one of the most powerful tools for studying the electronic density of states. However, there is, to the best of our knowledge, no valence photoemission datum for $Yb_{2.75}C_{60}$ yet. The reported valence photoemission spectra of Xia *et al.*[3] were for the Yb/C_{60} interface rather than $Yb_{2.75}C_{60}$. On the other hand, some reported works[4,5] have made it feasible now to study the valence-band structure of $Yb_{2.75}C_{60}$. Core-level x-ray photoemission (XPS) data[4] of a film sample showed that C_{60} mixing with Yb produced single-phase fulleride (the single phase was incorrectly determined to be Yb_2C_{60} in Ref. 4, and the actual composition of $Yb_{2.75}C_{60}$ was verified by the X-ray diffraction measurements[1]). The C 1*s* core level shifted to lower binding energy by ~0.4 eV as compared to pristine C_{60}. Thus the C 1*s* movement can be used as a sample characterization of $Yb_{2.75}C_{60}$. The near-edge x-ray absorption fine-structure (NEXAFS) measurements[5] exclusively indicated divalent Yb, which will help greatly in the analyses of the valence photoemission data. In this article, we report the ultraviolet photoelectron spectroscopy (UPS) measurements of $Yb_{2.75}C_{60}$ thin films.

Ultraviolet photoemission spectra for submonolayer C_{60} on a Yb thin film are also measured to study the electronic state evolutions of both C_{60} and Yb during their combination. The result can help to comprehend the electronic structure of $Yb_{2.75}C_{60}$. Although there was similar work reported in Ref. 3 for the C_{60}/Yb interface, we suspect the low-energy resolution (~0.4 eV) of the spectrometer used in Ref. 3 hindered the observations of some important information about the electronic states. Besides, the suggestion of mixed-valent Yb in Ref. 3 was in contradiction to the NEXAFS results.[5] The contradiction also indicates the necessity of in-depth studies of the Yb/C_{60} interface.

II. PREPARATION AND PES OF $Yb_{2.75}C_{60}$

A. Experiment

Sample preparations and measurements were performed in a multifunctional ultrahigh-vacuum VT-SPM-PES system (Omicron Instruments for Surface Science) with a base pressure better than 2×10^{-10} Torr. Samples were prepared in the preparation chamber and then transferred into the analyzer chamber for PES measurements. UPS measurements were performed with an uv lamp of He I (21.2 eV) and a sample bias of −5.0 V. XPS measurements were carried out with a Mg $K\alpha$ source (1253.6 eV). The overall energy resolutions were ~0.1 eV for UPS and ~0.9 eV for XPS respectively.

C_{60} and Yb were sublimed from Ta boats located ~11 cm away from the chemically etched silicon (B-doped) wafer substrate. Commercial C_{60} powder was first grown to be single crystals with the gas-phase method,[6] and then ground into powder by using an agate mortar. We carried out the above procedure to ensure the purity of the C_{60} raw material. The high-purity Yb (99.99%) was purchased from Beijing Research Institute for Nonferrous Metals. Low-energy electron diffraction (LEED) and XPS measurements were used to check the clean and well-ordered surfaces of all the substrates used in the present work. LEED patterns showed the clear and bright diffraction spots for the Si:H (111) surfaces. The O 1*s* and C 1*s* signals were negligible in the x-ray photoemission spectra. Before exposed to C_{60} or Yb, the sample holders and the substrates were thoroughly degassed at ~400 and ~250 °C, respectively.

The $Yb_{2.75}C_{60}$ phase was characterized by the C 1*s* core-level XPS measurements. The XPS data of Ohno *et al.*[4] were

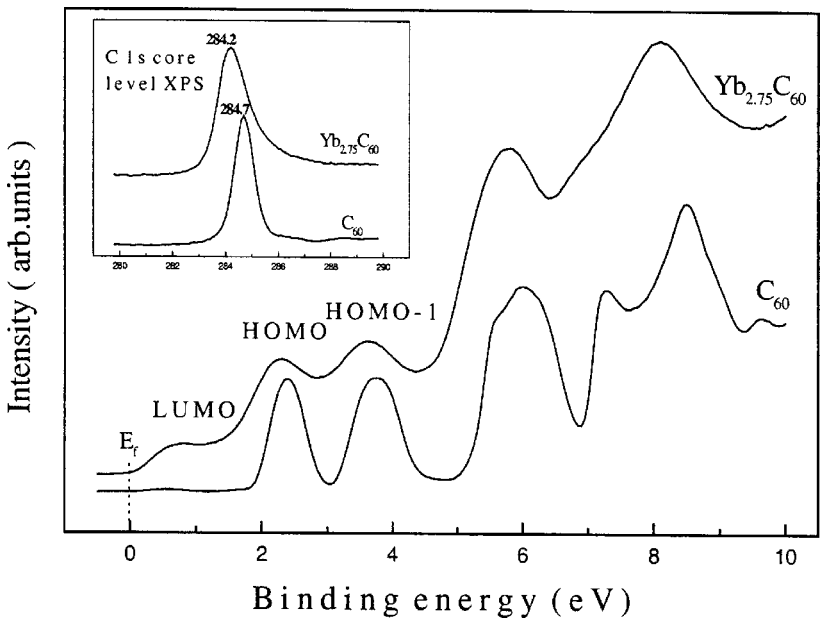

FIG. 1. Angular integrated ultraviolet photoemission spectra of $Yb_{2.75}C_{60}$ and pure C_{60} thin films. The data were taken at room temperature with the He I radiation. The two lines are normalized to the height of the HOMO peak. The insert exhibits the C 1*s* XPS peaks characterizing the $Yb_{2.75}C_{60}$ phase.

reproduced. As in Ref. 4, the C 1*s* core level shifted to lower binding energies until a homogeneous phase was obtained, and then shifted slightly to higher binding energies with excess Yb on the sample surface. The largest C 1*s* movement here is 0.5 eV, which is slightly larger than 0.4 eV in Ref. 4.

Then we prepared another sample. C_{60} thin film was prepared on the substrate at room temperature with thickness of ~200 Å as determined by using a quartz-crystal oscillator. During deposition of Yb, the sample was kept at 130 ± 5 °C. The doping procedure was step by step and the sample compositions were checked by XPS measurements after each doping period. Yb flux was fixed to be sufficiently small to obtain a homogeneous sample. It took eleven rounds (the Yb deposition time for each round was 20 min) for the homogeneous sample to form. Once the shift of C 1*s* had reached 0.5 eV, we ceased the deposition procedure and carried out the UPS measurements.

B. Results and discussions

The UPS and XPS results for the pure-phase sample are shown in Fig. 1 and the inset, respectively. Figure 1 also presents the spectral lines of the pristine C_{60} film for comparison. The position (near 2.4 eV) of the highest-occupied-molecular-orbital- (HOMO) derived band for pure C_{60} is consistent with other reported results.[7,8] Similar to the case of C_{60} doped with alkali or alkaline-earth-metal elements, the lowest-unoccupied-molecular-orbital- (LUMO) derived band appears (around 0.8 eV) below the Fermi level (E_F). This observation indicates that the electrons from the 6*s* states of Yb atoms move at least partly onto the C_{60} molecules due to the difference of electronegativities. A weak peak located near 0.6 eV can be seen in the spectral line of pure C_{60} due to the photoemission from the HOMO band stimulated by He I satellite radiation ($h\nu = 23.1$ eV, less than 2% intensity). Owing to the low intensity of the satellite radiation, its contribution to the observed LUMO spectral intensity of $Yb_{2.75}C_{60}$ can be neglected.

The dip between the LUMO band and the HOMO band is very shallow in Fig. 1. We argue that the shallow dip is partially due to the Yb $4f$ contribution as Yb $4f_{7/2}$ is located at ~1.2 eV with a relatively large photoionization cross section.[9] The real LUMO line shape may be represented by the dotted line in Fig. 2, which was obtained by subtracting the Yb $4f_{7/2}$ contribution from the experimental curve. The $4f_{7/2}$ contribution was simulated by a Gauss-type line located at 1.3 eV according to the XPS measurement[4] of the peak position for Yb $4f_{7/2}$ in $Yb_{2.75}C_{60}$. The full width at half maximum (FWHM) was taken to be that of the Yb metal film (see Sec. III). The integral intensity was determined by the photoionization cross sections of Yb $4f_{7/2}$ and C $2p$ (the calculated area ratio between the $4f_{7/2}$ and the combined HOMO and HOMO-1 was ~2.2%). Although there are some uncertainties in the simulation, Fig. 2 reveals that the $4f$ contribution is not negligible as compared to the LUMO signal. We believe the dotted line in Fig. 2 can be considered as a qualitative description of the LUMO band of $Yb_{2.75}C_{60}$, that is, a wide hump located between E_F and ~1.3 eV. The more accurate $4f$ contribution will be deduced by the PES studies with varying incident photon energies in future works.

The Fermi edge does not exist in Fig. 1 or Fig. 2. There is almost no photoemission at the Fermi level. If the superconductivity of $Yb_{2.75}C_{60}$ found by Özdas *et al.*[1] is further verified, $Yb_{2.75}C_{60}$ is, to the best of our knowledge, the unique superconducting fulleride found so far with semiconduction-like photoemission in normal states. (Takeuchi, Tanigaki, and Gogia argued that the superconducting phase could be Yb_4C_{60} in a conference report[2] and promised further studies. However, we have not yet seen any published subsequent works of the report.) For comparison, alkali-metal-doped superconducting A_3C_{60} (A=K,Rb) (Refs. 10 and 11) exhibited metal-like photoemissions.[12–15] Alkaline-earth-metal-doped superconducting Ca_5C_{60}, Sr_6C_{60} [or actually Sr_4C_{60} (Refs. 16 and 17)] and Ba_6C_{60} [or actually Ba_4C_{60} (Refs. 16 and

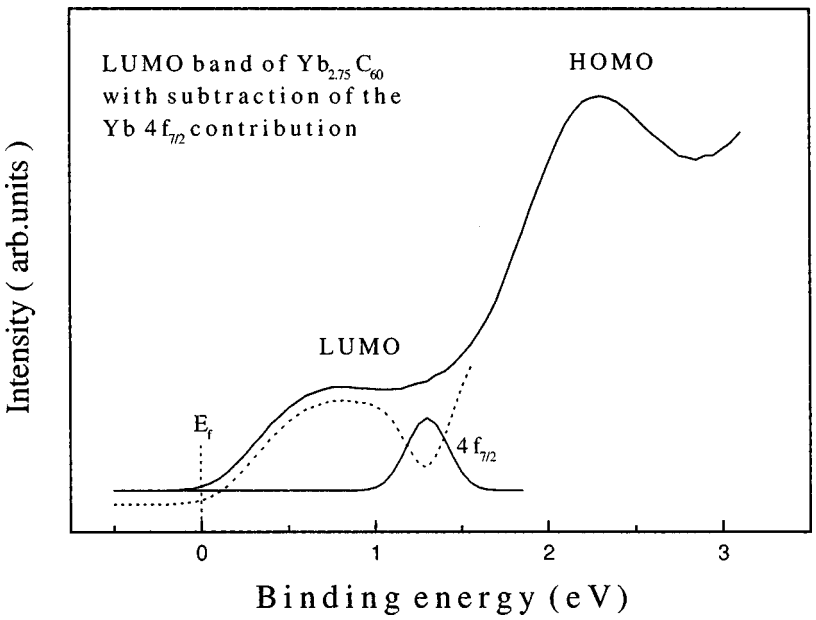

FIG. 2. Determination of the LUMO band of $Yb_{2.75}C_{60}$. The dotted line represents the LUMO band after subtracting the $4f_{7/2}$ contribution. The construction of the $4f_{7/2}$ UPS peak is described in the text.

17)] were also metallic or semimetallic in normal states.[18–24] Xia, Ruckman, and Strongin[3] and Ohno *et al.*[4] also found the semiconducting electronic property of $Yb_{2.75}C_{60}$ by the resistivity measurements in the temperature range from 10 to 400 K. However, the resistivity results[3,4] cannot readily deduce the observation of no Fermi edge in Fig. 1 due to the following reasons. First, the dependence of resistivity on temperature is sensitive to the sample preparation for fullerides. For example, the resistivity of K_3C_{60} polycrystalline sample decreased with increasing temperatures.[25] But the positive temperature coefficient of the resistivity for K_3C_{60} was found on single crystal[26] or high-qualified thin film[27] samples. Second, the narrow-band character of fullerides sometimes made a sample, e.g., Rb_1C_{60},[28] with notable photoemission at E_F show semiconducting resistivity. There is no simple relation between the resistivity behavior and the electronic state distribution at the Fermi level for the strongly correlated fullerides (the valence electrons of the fullerides are generally considered to be a strongly correlated system). On the other hand, one can predict readily the semiconducting property of $Yb_{2.75}C_{60}$ on the basis of the fact that no occupied electronic state is distributed at the Fermi level.

The results in Fig. 1 can also help us to give an estimation of the lower limit for the covalent contribution to the LUMO band on the basis of the atomic structure[1] and the partitioning of donated charge[5] of $Yb_{2.75}C_{60}$. $Yb_{2.75}C_{60}$ is believed to be neither the extreme covalent nor the extreme ionic fulleride. The C 1*s* core-level movements were considered to be the evidence of partial ionic contribution.[4] There was also evidence of Yb-C_{60} hybridization, such as the shortened Yb-C distance ($\sim$2.61 Å) being shorter than those in typically ionic Yb-C materials, the off-centered Yb cations, and the distortion of C_{60} anions.[1,5] However, there are debates on the importance of the covalent contribution.[1,3–5]

C_{60} anions have different charge although the Yb cations are electronically equivalent. The formal charge state of C_{60} in the fcc subcell is $(Yb^{2+})_{11}(C_{60}{}^{5.5-})_3(C_{60}{}^{4-})_{0.5}(C_{60}{}^{7-})_{0.5}$ due to three types of C_{60} in the subcell.[5] With the assumption of no charge transfer between C_{60} anions, the $C_{60}{}^{7-}$ charge state indicates the partial occupation of the LUMO+1 band. However, there is no evidence of the LUMO+1 filling in Fig. 1 (this assertion will be further supported by the UPS studies of Yb/C_{60} interface in Sec. III). The discrepancy is due to the existence of covalence. The Yb 6*s* electrons do not transfer completely to C_{60} [the so-called divalent Yb inferred from the NEXAFS data[5] specifies the Yb(II)($4f^{14}6s^2$) charge state, in contrast to Yb(III)($4f^{13}6s^2$), rather than the completely ionized Yb^{2+}]. The actual charge state of $Yb_{2.75}C_{60}$ should be $(Yb^{(2-\delta)+})_{11}(C_{60}{}^{2.75(2-\delta)-})_3(C_{60}{}^{2(2-\delta)-})_{0.5}(C_{60}{}^{3.5(2-\delta)-})_{0.5}$ as also proposed by Citrin *et al.*[5] The quantity of δ is a measurement of the covalent contribution. Based on Fig. 1, the value of $3.5(2-\delta)$ must be less than 6 (the largest electron number of the LUMO band), which gives the value of δ to be larger than 0.28. That is to say, more than 14% (=0.28/2) Yb 6*s* electrons are distributed in the Yb-C_{60} covalent bonds. Thus the result of Fig. 1 reveals the covalent contribution to the LUMO band is non-negligible. It must be mentioned, however, that the validity of the estimated lower limit (14%) depends on the rationality of the assumption of no charge transfer between C_{60} anions.

III. VALENCE-BAND EVOLUTION OF C_{60} ON Yb FILM

A. Experiment

A Yb thin film with thickness of $\sim$20 Å was prepared on the Si:H (111) surface at room temperature. Blurred LEED spots of the substrate could be seen at this coverage (a thickness of $\sim$30 Å could eliminate completely the substrate signals), which was in accordance with the escape depth of the electrons with energy of 35 eV (the energy value used in the LEED measurements). Two broad peaks from the Si:H-Yb interface were found at energies below 4.0 eV in the ultraviolet photoemission spectra. One of them located near 10.0 eV does not superimpose on the peaks of C_{60} or $Yb_{2.75}C_{60}$

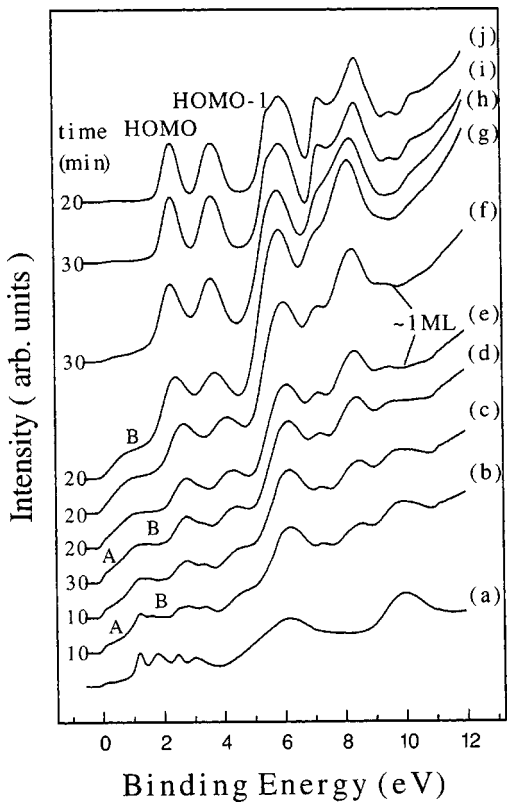

FIG. 3. Ultraviolet photoemission spectra of C_{60} deposited on Yb thin film. The bottom curve represents the UPS line of the Yb thin film prepared on the Si:H (111) substrate. The spectral intensities are normalized to the incident photon flux. Numbers aside each line exhibit the evaporating time of the C_{60} source for each deposition period. The amounts of the deposited C_{60} are estimated by the evaporating time. The symbols A and B emphasize there are two features (besides the Yb $4f$ features) between E_F and the HOMO feature.

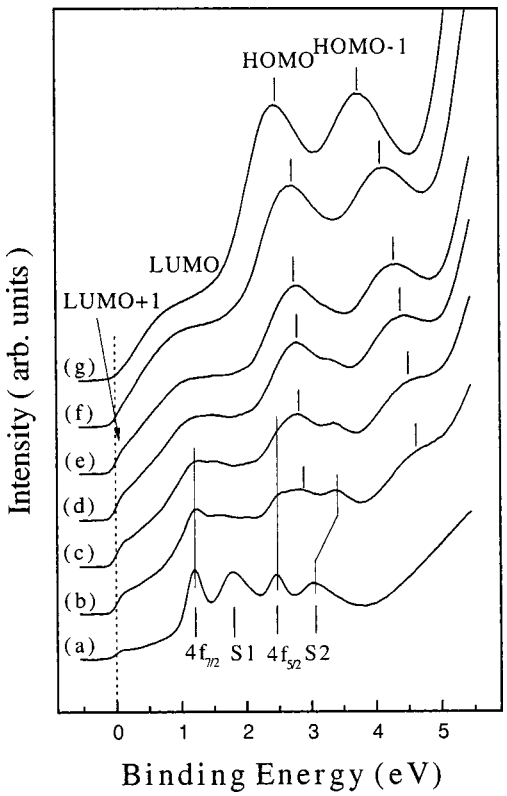

FIG. 4. Part of Fig. 3 to illustrate clearly the electronic state evolutions. Peak ascriptions are shown in the figure.

(see Fig. 1), and can be used as a more accurate reference than the quartz crystal oscillator to calibrate the amount of submonolayer C_{60}. For this reason, we did not use a thicker film to eliminate the Si:H-Yb interface photoemission. Besides, Si:H (111) surface has no photoemission between E_F and 1.5 eV, and has fairly weak photoemission between 1.5 and 4.0 eV. Thus the Si:H-Yb interface photoemission signals do not affect the analyses of the interactions between Yb and C_{60}.

C_{60} was deposited onto the Yb film at a very low flux as only one monolayer (ML) C_{60} could make the UPS signals from the covered materials vanish.[29,30] The amount of C_{60} for each round was estimated by the evaporating time. (The electric current through the Ta boat was fixed at the same value for all rounds. See below for more details.) The Yb film was kept at room temperature during the C_{60} depositions.

B. Results and discussions

The UPS data are shown in Fig. 3. Part of the figure is enlarged in Fig. 4 to clarify the valence evolution. Curve (a) exhibits the clear Fermi edge of the metal Yb $6s$ band. Two peaks at ~1.2 and ~2.5 eV are derived from the $4f_{7/2}$ and $4f_{5/2}$ doublet,[31] and the two peaks labeled with S1 and S2 are the surface states of Yb film with sufficient thickness.[31,32] Two broad peaks near 6.0 and 10.0 eV are derived from the Si:H-Yb interface as mentioned above. The C_{60} deposition time for each round is shown next to the lines in Fig. 3. After four (or five) rounds of deposition, the Si:H-Yb signal near 10.0 eV disappears. Thus curves (e) and (f) represent the UPS data of ~1 ML C_{60} on the Yb film with the assumption of no stacking [scanning tunneling microscopy (STM) results[33,34] indeed revealed the discrete C_{60} molecules on the substrate surfaces below the coverage of 1 ML]. Then the amount of C_{60} per 10 min deposition is estimated to be ~1/8 ML.

During the deposition of C_{60}, the spectrum becomes complicated. Many new peaks emerge. These peaks change their positions obviously with successive depositions. The $4f_{7/2}$ and $4f_{5/2}$ positions keep unvaried corresponding to the localized inner $4f^{14}$ shell of the divalent Yb.[5,35] The S1 peak weakens and S2 peak shifts to higher binding energy by ~0.3 eV due to their surface sensitivity. There are two features (besides the $4f$ features) labeled A and B between the Fermi level and the HOMO feature from curve (b) through curve (e). The abundant spectral information in Fig. 3 cannot only help us understand the electronic structure of $Yb_{2.75}C_{60}$, but also exhibits the electronic properties of submonolayer C_{60} on Yb metal, which is different from that of $Yb_{2.75}C_{60}$.

The new peaks at ~2.9 and 4.6 eV, and some higher binding energies in curve (b), can be easily ascribed to the C_{60} UPS features by the inspection of the electronic state evolu-

tion from curve (a) through curve (j). Compared to the pure C_{60} [Fig. 1 or curve (j) in Fig. 3], most of these peaks shift to higher binding energies. Xia, Ruckman, and Strongin[3] reached the possible conclusion that Yb at the Yb/C_{60} interface was mixed valent on the basis of the emergency of a new peak (the G peak in Ref. 3) near 5 eV in the ultraviolet photoemission spectrum for 1 Å C_{60} deposited on a Yb thick film. They argued this peak originated from the $4f^{13}$ configuration. This peak is also observed at ~4.6 eV in Fig. 4(b). However, it is actually the HOMO−1 band, as is very evident by the inspection of the peak evolutions from curve (b) through curve (f). Thus, the very precise deposition process in this work reveals that there is actually no contradiction between the results of UPS and NEXAFS studies.[3,5]

The spectral weight at the Fermi level increases substantially in curve (b) as compared to curve (a). This observation indicates the $2p$ π-like states of C_{60} are occupied due to the fact that the photoionization cross section of C $2p$ is ~100 times of that for the Yb $6s$ state.[9] Taking into account the small amount (~1/8 ML) of C_{60} on the Yb film, we can say that the $6s$ electrons can easily transfer from Yb to C_{60}. This observation unambiguously reveals the LUMO band of $Yb_{2.75}C_{60}$ (Fig. 1) should have large ionic contribution. We deduced the lower limit of ~14% for the covalent contribution to the Yb-C_{60} bonding in Sec. II. The result in Fig. 3 indicates the upper limit should not be large. The bonding of $Yb_{2.75}C_{60}$ is mainly ionic with some covalent contribution.

There are two possible origins for the two features between the Fermi level and the HOMO peak in the lower lines in Fig. 3. First, the LUMO+1 orbital of C_{60} is partially occupied. Second, the LUMO orbital splits due to the asymmetry environment around the C_{60} molecule. The latter scenario cannot interpret the combined intensity of features A and B as compared to that of the HOMO feature. The former should be close to $\frac{3}{5}$ times of the latter in this scenario by considering the degeneracies of LUMO (threefold) and HOMO (fivefold). However, the combined intensity of features A and B is no less than that of the HOMO feature in curves (b) and (c). Thus we can conclude that the LUMO +1 orbital of C_{60} is partially filled at submonolayer coverage. Features A and B originate from the LUMO+1 and LUMO states of C_{60}, respectively, as labeled in Fig. 4. The LUMO+1 band filling was observed in alkaline-earth-metal-doped fullerides and was responsible for the superconductivity.[18] Although it is not occupied in $Yb_{2.75}C_{60}$, the LUMO+1 orbital can be occupied at the C_{60}-Yb interface with low C_{60} coverage due to the large number of Yb atoms around one C_{60} molecule.

The above ascriptions of features A and B can reasonably explain the peak movements and the valence evolutions in Fig. 4. With successive deposition of C_{60}, the average number of Yb atoms around each C_{60} and the number of electrons occupying the LUMO+1 orbital decrease. The Fermi level moves towards LUMO feature, i.e., LUMO feature together with the HOMO and HOMO−1 features moves to E_f as can be seen in Fig. 4. The integral intensity of the LUMO+1 feature decreases from curve (b) through curve (e) in Fig. 4, but the Fermi edge still exists due to the partial occupation. With the coverage of ~1 ML C_{60}, the LUMO+1 feature has little spectral weight in curve (f). It disappears completely in curve (g). By the way, the line shape of curve (g) is somewhat analogous to that of $Yb_{2.75}C_{60}$ (Fig. 1), which further supports our assertion in Sec. II that the LUMO+1 band in $Yb_{2.75}C_{60}$ is not occupied. More depositions of C_{60} rapidly eliminate the LUMO photoemission and produce the ultraviolet photoemission spectrum of pure C_{60}.

IV. CONCLUSIONS

In summary, we acquire the density of states near the Fermi level of $Yb_{2.75}C_{60}$, which will play important roles in the studies of the superconducting mechanism and other physical properties. $Yb_{2.75}C_{60}$ is semiconducting as there is no Fermi edge in the ultraviolet photoemission spectrum. The Yb-C_{60} bonding in $Yb_{2.75}C_{60}$ is mainly ionic with some covalent contributions. A value of 14% is estimated to be the lower limit of the covalent contribution. LUMO+1 orbital of C_{60} can be partially occupied at low coverage of C_{60} on Yb film. There is no photoemission evidence of trivalent Yb in $Yb_{2.75}C_{60}$.

ACKNOWLEDGMENTS

This work was supported by the National Natural Science Foundation of China under Grant No. 10074053 and the Zhejiang Provincial Natural Science Foundation under Grant No. 100019.

[1] E. Özdas, A. R. Kortan, N. Kopylov, A. P. Ramirez, T. Siegrist, K. M. Rabe, H. E. Bair, S. Schuppler, and P. H. Citrin, Nature (London) **375**, 126 (1995).

[2] J. Takeuchi, K. Tanigaki, and B. Gogia, in *Nanonetwork Materials: Fullerenes, Nanotubes, and Related Systems*, edited by S. Saito, T. Ando, Y. Iwasa, K. Kikuchi, M. Kobayashi, and Y. Saito, AIP Conf. Proc. No. 590 (AIP, New York, 2001), p. 361.

[3] Bo Xia, M. W. Ruckman, and Myron Strongin, Phys. Rev. B **48**, 14 623 (1993).

[4] T. R. Ohno, G. H. Kroll, J. H. Weaver, L. P. F. Chibante, and R. E. Smalley, Phys. Rev. B **46**, 10 437 (1992).

[5] P. H. Citrin, E. Özdas, S. Schuppler, A. R. Kortan, and K. B. Lyons, Phys. Rev. B **56**, 5213 (1997).

[6] Hongnian Li, Yabo Xu, Jianhua Zhang, Peimo He, Haiyang Li, Taiquan Wu, and Shining Bao, Prog. Nat. Sci. **11**, 427 (2001).

[7] Th. Schedel-Niedrig, M. C. Böhm, H. Werner, J. Schulte, and R. Schlögl, Phys. Rev. B **55**, 13 542 (1997).

[8] M. Merkel, M. Knupfer, M. S. Golden, J. Fink, R. Seemann, and R. L. Johnson, Phys. Rev. B **47**, 11 470 (1993).

[9] J. J. Yeh and I. Lindau, *Atomic Subshell Photoionization Cross Section and Asymmetry Parameters*: $1 \leqslant Z \leqslant 103$ (Academic, New York, 1985), pp. 7–11.

[10] A. F. Hebard, M. J. Rosseinsky, R. C. Haddon, D. W. Murphy, S. H. Glarum, T. T. M. Palstra, A. P. Ramirez, and A. R. Kortan,

Nature (London) **350**, 600 (1991).
[11] M. J. Rosseinsky, A. P. Ramirez, S. H. Glarum, D. W. Murphy, R. C. Haddon, A. F. Hebard, T. T. M. Palstra, A. R. Kortan, S. M. Zahurak, and A. V. Makhija, Phys. Rev. Lett. **66**, 2830 (1991).
[12] A. Goldoni, S. L. Friedmann, Z.-X. Shen, M. Peloi, F. Parmigiani, G. Comelli, and G. Paolucci, J. Chem. Phys. **113**, 8266 (2000).
[13] R. Hesper, L. H. Tjeng, A. Heeres, and G. A. Sawatzky, Phys. Rev. B **62**, 16 046 (2000).
[14] T. Takahashi, T. Morikawa, S. Hasegawa, K. Kamiya, H. Fujimoto, S. Hino, K. Seki, H. Katayama-Yoshida, H. Inokuchi, K. Kikuchi, S. Suzuki, K. Ikemoto, and Y. Achiba, Physica C **190**, 205 (1992).
[15] Chun Gu, B. W. Veal, R. Liu, A. P. Paulikas, P. Kostic, H. Ding, K. Gofrom, J. C. Campuzano, J. A. Schlueter, H. H. Wang, U. Geiser, and J. M. Williams, Phys. Rev. B **50**, 16 566 (1994).
[16] M. Baenitz, M. Heinze, K. Lüders, H. Werner, R. Schlögl, M. Weiden, G. Spam, and F. Steglich, Solid State Commun. **96**, 539 (1995).
[17] B. Gogia, K. Kordatos, H. Suematsu, K. Tanigaki, and K. Prassides, Phys. Rev. B **58**, 1077 (1998).
[18] G. K. Wertheim, D. N. E. Buchanan, and J. E. Rowe, Science **258**, 1638 (1992).
[19] M. Knupfer, F. Stepniak, and J. H. Weaver, Phys. Rev. B **49**, 7620 (1994).
[20] S. Saito and A. Oshiyama, J. Phys. Chem. Solids **54**, 1759 (1993).
[21] G. K. Wertheim and D. N. E. Buchanan, J. Phys. Chem. Solids **56**, 745 (1995).
[22] R. C. Haddon, G. P. Kochanski, A. F. Hebard, A. T. Fiory, and R. C. Morris, Science **258**, 1636 (1992).
[23] R. C. Haddon, G. P. Kochanski, A. F. Hebard, A. T. Fiory, R. C. Morris, and A. S. Perel, Chem. Phys. Lett. **203**, 433 (1993).
[24] Y. Chen, D. M. Porier, M. B. Jost, C. Gu, T. R. Ohno, J. L. Matins, J. H. Weaver, L. P. F. Chibante, and R. E. Smalley, Phys. Rev. B **46**, 7961 (1992).
[25] S. K. Watson, K. Allen, D. W. Denlinger, and F. Hellman, Phys. Rev. B **55**, 3866 (1992).
[26] J. G. Hou, L. Liu, V. H. Crespi, X.-D. Xiang, A. Zettl, and M. L. Coher, Solid State Commun. **93**, 973 (1995).
[27] A. Goldoni, L. Sangaletti, F. Parmigiani, G. Comelli, and G. Paolucci, Phys. Rev. Lett. **87**, 076401 (2001).
[28] P. J. Benning, F. Stepniak, and J. H. Weaver, Phys. Rev. B **48**, 9086 (1993).
[29] L. H. Tjeng, R. Hesper, A. C. L. Heessels, A. Heeres, H. T. Jonkman, and G. A. Sawataky, Solid State Commun. **103**, 31 (1997).
[30] B. W. Hoogenboom, R. Hesper, L. H. Tjeng, and G. A. Sawatzky, Phys. Rev. B **57**, 11 939 (1998).
[31] E. Weschke, G. Kaindl, J. Electron Spectrosc. Relat. Phenom. **75**, 233 (2001).
[32] G. Kaindl, A. Höhr, E. Weschke, S. Vandre, C. Schüßler-Langeheine, and C. Laubschat, Phys. Rev. B **51**, 7920 (1995).
[33] Y. Z. Li, M. Chander, J. C. Patrin, J. H. Weaver, L. P. F. Chibante, and R. E. Smalley, Phys. Rev. B **45**, 13 837 (1992).
[34] S. Saito, K. Sakamoto, D. Kondo, T. Wakita, A. Kimura, A. Kakizaki, C.-W. Hu, A. Kasuyu, Surf. Sci. **438**, 242 (1999).
[35] A. Svane, W. M. Temmerman, Z. Szotek, L. Petit, P. Strange, and H. Winter, Phys. Rev. B **62**, 13 394 (2000).